PHYSOR 2004- *The Physics of Fuel Cycles and Advanced Nuclear Systems: Global developments*
Chicago, Illinois, April 25-29, 2004, on CD-ROM, American Nuclear Society, Lagrange Park, IL. (2004)

Mixed-Hybrid Methods for the Linear Transport Equation

S. Van Criekingen *[1], E.E. Lewis[1] and R.Beauwens[2]

[1] *Northwestern University, Mechanical Eng. Dept., Evanston, IL 60208, U.S.A.*

[2] *Free University of Brussels, Nuclear Metrology Dept., Brussels, Belgium*

Mixed-hybrid methods generalize the existing mixed and hybrid methods combining their attractive features. A significant achievement is that not only odd- but also even-parity P_N approximations are used for the angular discretization. This leads to a promising enclosing property in our numerical tests. Furthermore, we establish flux and current interface continuity properties from the Rumyantsev conditions, for which we outline a new derivation.

KEYWORDS: Boltzmann transport equation, Mixed-hybrid methods, Spherical harmonics, Rumyantsev conditions

1 Introduction

Mixed-hybrid methods are here applied to the solution of the within-group linear Boltzmann transport equation, where isotropic scattering and sources are assumed. A finite element technique is used for the spatial discretization, while a P_N spherical harmonics technique is used for the angular discretization. Unlike the alternative S_N discrete ordinates approach, the P_N approach does not exhibit ray effects [1, pp.194-203].

Second order, mixed, hybrid, and mixed-hybrid transport methods are based on the even- and odd- (angular) parity flux decomposition due to Vladimirov [2]. Depending on the role played by the even- and odd-parity fluxes, these methods can be cast into a primal or a dual formulation. Hybrid methods are characterized by the use of Lagrange multipliers to enforce interface continuity properties, and mixed methods by their leading to simultaneous independent approximations of even- and odd- parity fluxes (thus of flux and current). Mixed-hybrid methods are both mixed and hybrid. While their study also provides insight for purely hybrid and purely mixed methods, these methods can be used as such [3].

Second order (EVENT code [4]) and hybrid (VARIANT code [5]) transport methods have been widely applied to reactor physics problems utilizing odd-order spherical harmonics approximations in angle. Mixed methods however have only been developed thus far in the diffusion approximation (CRONOS/MINOS code [6]) or simplified spherical harmonics, using Raviart-Thomas finite elements in space. These elements can not be used in the transport case. The mixed-hybrid methods presented in this work provide a way

*Corresponding author, svancrie@northwestern.edu

to generalize mixed methods to the transport equation, through hybridization. This work also generalizes the hybrid method of VARIANT [5] to a mixed formulation, considering internal as well as interface flux and currents.

Furthermore, we demonstrate the application of mixed-hybrid methods to even- as well as odd-order P_N spherical harmonics approximations to the transport equation. Up to now, even-order P_N approximations have been for the most part neglected. Also, we emphasize the flux and current interface continuity properties.

For brevity, we concentrate here on the primal case. The paper starts with the primal mixed-hybrid weak form derivation in section 2. Section 3 is concerned with the discretized problem. The interface angular expansions derived in §3.1 correspond to the Rumyantsev conditions [7], for which we outline a new derivation. In turn, continuity properties are discussed in section 3.2. Finally, numerical results are displayed in section 4, showing a promising enclosing behavior when both even- and odd- order P_N methods are used.

2 Mixed-Hybrid Weak Forms

The transport equation for the angular flux $\Psi(\mathbf{r},\mathbf{\Omega})$ that we consider reads

$$\mathbf{\Omega}\cdot\nabla\Psi(\mathbf{r},\mathbf{\Omega})+\sigma(\mathbf{r})\Psi(\mathbf{r},\mathbf{\Omega})=\sigma_s(\mathbf{r})\phi(\mathbf{r})+s(\mathbf{r})$$

where $\phi(\mathbf{r})=\int_S d\mathbf{\Omega}\Psi(\mathbf{r},\mathbf{\Omega})$ is the scalar flux, σ and σ_s are the macroscopic total and isotropic scattering cross sections, s is the isotropic source, and S represents the unit sphere. The even- and odd-parity decomposition [2] for the angular flux $\Psi^{\pm}(\mathbf{r},\mathbf{\Omega})=\frac{1}{2}\left(\Psi(\mathbf{r},\mathbf{\Omega})\pm\Psi(\mathbf{r},-\mathbf{\Omega})\right)$ yields the following coupled pair of first order equations:

$$\mathbf{\Omega}\cdot\nabla\Psi^{-}(\mathbf{r},\mathbf{\Omega})+\sigma\Psi^{+}(\mathbf{r},\mathbf{\Omega})=\sigma_s\phi(\mathbf{r})+s(\mathbf{r}) \tag{1}$$

$$\mathbf{\Omega}\cdot\nabla\Psi^{+}(\mathbf{r},\mathbf{\Omega})+\sigma\Psi^{-}(\mathbf{r},\mathbf{\Omega})=0. \tag{2}$$

To derive the weak form equations, we multiply the equations (1) and (2) by test functions $\tilde{\Psi}^{+}(\mathbf{r},\mathbf{\Omega})$ and $\tilde{\Psi}^{-}(\mathbf{r},\mathbf{\Omega})$. Integrating over space and angle, and applying the divergence theorem to the first equation, we obtain:

$$-\int_S d\mathbf{\Omega}\int_V dV\,\mathbf{\Omega}\cdot\nabla\tilde{\Psi}^{+}\Psi^{-}+\int_S d\mathbf{\Omega}\int_{\partial V} d\Gamma\,\mathbf{\Omega}\cdot\mathbf{n}\,\tilde{\Psi}^{+}\Psi^{\chi}+\int_S d\mathbf{\Omega}\int_V dV\sigma\,\tilde{\Psi}^{+}\Psi^{+}$$
$$-\int_S d\mathbf{\Omega}\int_V dV\left(\sigma_s\tilde{\Psi}^{+}\int_S d\Omega'\Psi^{+}\right)=\int_S d\mathbf{\Omega}\int_V dV\,s\,\tilde{\Psi}^{+}\,,\quad\text{and}$$
$$\int_S d\mathbf{\Omega}\int_V dV\tilde{\Psi}^{-}\left(\mathbf{\Omega}\cdot\nabla\Psi^{+}+\sigma\Psi^{-}\right)=0$$

where $\Psi^{\chi}(\mathbf{\Omega},\mathbf{r})$ represents the value of Ψ^{-} on the boundary ∂V of the spatial domain V. In a hybrid method, this domain is subdivided into a finite family of non-overlapping elements (or nodes) V_l, and we keep only weak (but natural) regularity conditions at the interfaces of the spatially decomposed domain. In this view, we restrict the above equations to $S\times V_l$

(that is spatial integrations are now taken on V_l and ∂V_l), and sum them up. Using a subscript l to denote restrictions to $S \times V_l$, the mixed-hybrid primal weak form equations are

$$\sum_l \Big[- \int_S d\mathbf{\Omega} \int_{V_l} dV\, \Psi_l^- \, \mathbf{\Omega} \cdot \nabla \tilde{\Psi}_l^+ + \int_S d\mathbf{\Omega} \int_{\partial V_l} d\Gamma\, \mathbf{\Omega} \cdot \mathbf{n}\, \tilde{\Psi}_l^+ \Psi_l^\chi + \int_S d\mathbf{\Omega} \int_{V_l} dV \sigma_l \tilde{\Psi}_l^+ \Psi_l^+ - \int_S d\mathbf{\Omega} \int_{V_l} dV \Big(\sigma_{s,l} \tilde{\Psi}_l^+ \int_S d\Omega' \Psi_l^+ \Big) \Big] = \sum_l \int_S d\mathbf{\Omega} \int_{V_l} dV\, s\, \tilde{\Psi}_l^+ \tag{3}$$

$$\sum_l \left[\int_S d\mathbf{\Omega} \int_{V_l} dV \tilde{\Psi}_l^- \mathbf{\Omega} \cdot \nabla \Psi_l^+ + \int_S d\mathbf{\Omega} \int_{V_l} dV \sigma_l \tilde{\Psi}_l^- \Psi_l^- \right] = 0 \tag{4}$$

$$\sum_l \left[\int_S d\mathbf{\Omega} \int_{\partial V_l \setminus \partial V} d\Gamma\, \mathbf{\Omega} \cdot \mathbf{n}\, \tilde{\Psi}_l^\chi \Psi_l^+ \right] = 0, \tag{5}$$

where a third equation involving the Lagrange multiplier $\tilde{\Psi}^\chi$ was added to enforce weak natural interface regularity conditions for Ψ^+. This last equation acts on any interface between two elements V_l, but not on the external boundary ∂V. We thus look for Ψ^+, Ψ^-, and Ψ^χ such that the weak form equations are verified for any test functions $\tilde{\Psi}^+, \tilde{\Psi}^-$, and $\tilde{\Psi}^\chi$ in suitable spaces. Note that Ψ^χ is here an interface unknown defined on $\bigcup_l \partial V_l$ (including the external boundary ∂V).

Using the divergence theorem in the second equation instead of the first, leads similarly to the mixed-hybrid dual weak form.

3 Space-Angle discretization

To write the complete discretization of Ψ^+, Ψ^- and Ψ^χ we need to introduce both spatial and angular discretizations. Our treatment is inspired by [5].

For the spatial discretization, we apply a finite element method as in [5]. Inside each element V_l (i.e. for $\Psi^\pm$), we take polynomial expansions cast into a (column) vector $f_{\pm,l}(\mathbf{r})$. On interfaces (i.e. for Ψ^χ), we take polynomial expansions cast into a vector $h_i(\mathbf{r})$, where the subscript i refers to the edge i of the element V_l. We consider here regular convex union-of-rectangle domains. Also, these polynomials are taken nonzero only on the considered (edge i of the) element V_l, and such that the obtained bases are orthonormal.

For the angular discretization, we use a P_N spherical harmonics method. We introduce the vectors of spherical harmonics $y_{\pm,l}(\mathbf{\Omega})$ to expand the angular dependence of the internal unknowns $\Psi^\pm$. These basis vectors are built as in [5], that is with the real and imaginary parts of the spherical harmonics. Given their parity properties, we take

$$\begin{aligned} y_{+,l}^T(\mathbf{\Omega}) &= (Y_{00}, Y_{20}, Y_{2\pm1}, Y_{2\pm2}, Y_{40}, Y_{4\pm1}, Y_{4\pm2}, Y_{4\pm3}, Y_{4\pm4}, Y_{60} \ldots), \text{ and} \\ y_{-,l}^T(\mathbf{\Omega}) &= (Y_{10}, Y_{1\pm1}, Y_{30}, Y_{3\pm1}, Y_{3\pm2}, Y_{3\pm3}, Y_{50}, \ldots), \end{aligned}$$

where $Y_{l\pm m}$ means that both Y_{lm} (cosine series) and Y_{l-m} (sine series) are separately present in the vector. Truncating this expansion for $l = N$ gives the P_N approximation. As for the interface unknown Ψ^χ, its angular dependence is expanded using the vector of spherical harmonics $y_\chi(\mathbf{\Omega})$. This basis vector differs from the one presented in [5], and section (3.1) is devoted to its derivation.

The spatial and angular expansions are coupled through the Kronecker product. Thus, inside each V_l and on an edge i, we end up with the approximations

$$\Psi_l^\pm(\mathbf{r},\mathbf{\Omega}) \approx \left[y_{\pm,l}^T(\mathbf{\Omega}) \otimes f_{\pm,l}^T(\mathbf{r})\right]\ \varphi_l^\pm \quad \text{and} \quad \Psi_i^\chi \approx \left[y_{\chi,i}^T(\mathbf{\Omega}) \otimes h_i^T(\mathbf{r})\right]\chi_i,$$

where $\varphi_l^\pm$ and χ_i are the coefficient column vectors to be determined. As for test functions, we take them equal to the transposed expansion functions.

3.1 *Interface Angular Expansions*

We now establish the appropriate interface angular basis y_χ. The weak form equations (3) and (5) contain an interface integral whose angular part yields the matrix

$$\int_S d\mathbf{\Omega}\ \mathbf{\Omega}\cdot\mathbf{n}\ y_+\, y_\chi^T \tag{6}$$

where the y_+ elements are already determined. The y_χ must be chosen such that this matrix is of full rank. This choice is not unique. One was developed in [8, appendix A]. Another one, taken here, leads to the Rumyantsev conditions. In fact, we choose the y_χ elements by combining the (odd-parity) Y_{lm} that make the entries of (6) non-zero for each given y_+ element. This can be done using spherical harmonics properties (Wigner coefficients) and will be detailed in a later publication. We here reproduce the conclusions for the approximations P_1 to P_5. The odd-parity interface angular bases read as follows:

$$\begin{aligned}
P1 &: y_\chi = (Y_{10}),\\
P2 &: y_\chi = (Y_{10}, Y_{1\pm1}),\\
P3 &: y_\chi = (Y_{10}, Y_{30}, Y_{1\pm1} + \sqrt{\frac{8}{7}}Y_{3\pm1}, Y_{3\pm2}),\\
P4 &: y_\chi = (Y_{10}, Y_{1\pm1}, Y_{30}, Y_{3\pm1}, Y_{3\pm2}, Y_{3\pm3}),\\
P5 &: y_\chi = (Y_{10}, Y_{30}, Y_{1\pm1} + \sqrt{\frac{8}{7}}Y_{3\pm1}, Y_{3\pm2}, Y_{50}, \sqrt{\frac{15}{7}}Y_{3\pm1} + 2\sqrt{\frac{6}{11}}Y_{5\pm1},\\
&\quad Y_{5\pm2}, Y_{3\pm3} + \frac{4}{\sqrt{11}}Y_{5\pm3}, Y_{5\pm4}).
\end{aligned}$$

These expansions are known as the Rumyantsev conditions [7] in the literature. Their present form has first been derived in a work by Yang [9], based on [7]. The derivation procedure outlined here is different, but leads to the same result.

Treating the dual case yields the even-parity interface angular bases, that also appear in the next section.

3.2 *Interface Continuity Properties*

As stated earlier, the interface continuity (with respect to the $\mathbf{r}$ variable) of Ψ^+ is enforced through the third equation (5) of the weak form. Nevertheless, this continuity, although guaranteed in infinite-dimensional spaces, is only partly achieved after discretization. We concentrate here on the consequences of using truncated angular expansions. We denote by N_+, N_- and N_χ respectively the lengths of y_+, y_- and y_χ. Then for even-order P_N approximations, $y_\chi = y_-$ and $N_\chi = N_- < N_+$, while for odd-order P_N approximations, $y_\chi \neq y_-$ and $N_\chi = N_+ < N_-$.

Now that the y_χ elements are established, note that the angular part of equation (5), given by (6), provides only N_χ relations. Hence, if $N_\chi < N_+$, equation (5) does not provide enough equations to enforce the continuity of all the Ψ^+ angular components. This happens in even-order primal methods, but not in odd–order primal methods. We next introduce y_ψ as the vector containing the $N_\chi = N_\psi$ [a] combinations of (even-parity) Y_{lm} that make the entries of the matrix

$$\int_S d\mathbf{\Omega}\, \mathbf{\Omega} \cdot \mathbf{n}\, y_\psi\, y_\chi^T$$

non-zero for each given y_χ element. The y_ψ elements are then the Ψ^+ angular components that can actually be enforced continuous at interfaces. They can again be determined using spherical harmonics properties, yielding the following even-parity interface angular bases for the first P_N approximations:

$$\begin{aligned}
P1 &: y_\psi = (Y_{00}),\\
P2 &: y_\psi = (Y_{00} + \frac{2}{\sqrt{5}}Y_{20}, Y_{2\pm1}),\\
P3 &: y_\psi = (Y_{00}, Y_{20}, Y_{2\pm1}, Y_{2\pm2}),\\
P4 &: y_\psi = (Y_{00} + \frac{2}{\sqrt{5}}Y_{20}, Y_{2\pm1}, \frac{3}{\sqrt{5}}Y_{20} + \frac{4}{3}Y_{40}, Y_{4\pm1}, Y_{2\pm2} + \frac{2}{\sqrt{3}}Y_{4\pm2}, Y_{4\pm3}),\\
P5 &: y_\psi = (Y_{00}, Y_{20}, Y_{2\pm1}, Y_{2\pm2}, Y_{40}, Y_{4\pm1}, Y_{4\pm2}, Y_{4\pm3}, Y_{4\pm4}).
\end{aligned}$$

In odd-order primal methods, $y_\psi = y_+$ and the interface continuity of all the Ψ^+ angular components can be enforced. In even-order methods, $y_\psi \neq y_+$ and only the y_ψ elements can be enforced continuous. Thus in any primal method, y_ψ spans all the continuous Ψ^+ components.

As for the continuity of Ψ^-, since its interface value equals Ψ^χ, only the components of Ψ^- spanned by y_χ (given in section 3.1) match on both sides of an interface edge. Thus, in any primal method, y_χ spans all the continuous Ψ^- components.

In reactor physics applications, the most valuable quantities are the Y_{00}, Y_{10} and $Y_{1\pm1}$ components, corresponding to the scalar flux ϕ (Y_{00}) and the current vector $\mathbf{J}$ (with our conventions, Y_{10} corresponds to the normal current, and $Y_{1\pm1}$ to the two components of the parallel current (in three dimensions)). Developments in section 3.1 show that y_ψ contains

[a] N_ψ denotes the length of y_ψ

Y_{00} on its own only when N is odd, y_χ contains Y_{10} on its own regardless of the parity of N, and y_χ contains $Y_{1\pm1}$ on its own only when N is even. Consequently, we can say that for our primal mixed-hybrid methods,

- in odd-order P_N methods, the continuity of the flux and normal current, but not the continuity of the parallel current, can be enforced at interfaces,
- in even-order P_N methods, the continuity of the normal and parallel currents, but not the continuity of the flux, can be enforced at interfaces.

The analysis of the dual case leads to the same conclusions for the interface continuity. Note that the continuity of the normal current is required in order to ensure neutron conservation properties within each element V_l.

4 Numerical Results

The primal and dual discrete weak forms are both applicable with an even- or odd-order P_N approximation. We here plot results obtained using even- and odd-order primal methods. Dual results are similar to the primal ones.

Our methods have been tested on the 2D iron-water benchmark problem, whose geometry is recalled in figure 1. Zones 1, 2 and 3 respectively correspond to water with source,

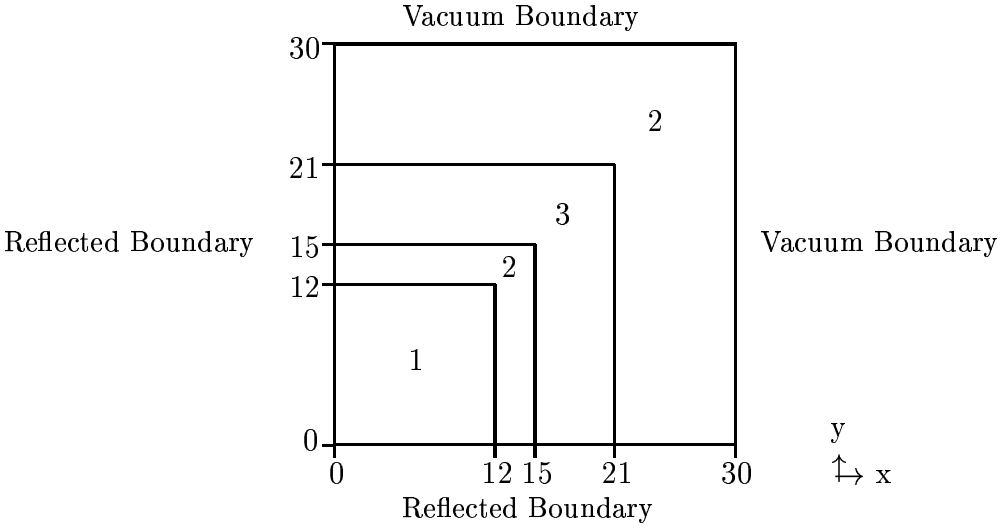

Figure 1: Iron-water Benchmark Geometry

water alone, and iron. Cross-section for these zones are given in [10]. Note that in two dimensions, symmetry eliminates the Y_{lm} with negative m from the angular expansions. The linear matrix system was solved using a standard MATLAB routine ("minres", a minimum residual technique) as a black box. A 30×30 grid was used together with a fixed

spatial polynomial expansion order, namely sixth order within each V_l (i.e. for $f_{\pm,l}(\mathbf{r})$) [b], and second order on interfaces (i.e. for $h_i(\mathbf{r})$).

The primal flux at $y = 29.75$ (i.e. close to the vacuum boundary), is plotted on figure 2. We notice on the zoom that the even-parity P_N methods approximate from above, while the odd-parity P_N methods approximate from below. Such enclosing property appears repeatedly, also in the dual case.

To illustrate the continuity properties discussed in §3.2, primal flux (figure 3) and current (figure 4) are plotted at $y = 7.5$. We zoom on the discontinuities arising at $x = 15$. We verify on figure 3 that the even-order methods cannot ensure the continuity of the flux, and on figure 4 that odd-order methods cannot ensure the continuity of the parallel current $J_{\|}$, that is here the Y-current. Note that the enclosing property is visible on these plots as well, i.e. the even-order P_N methods approximate from above when odd-order P_N methods approximate from below, and vice-versa.

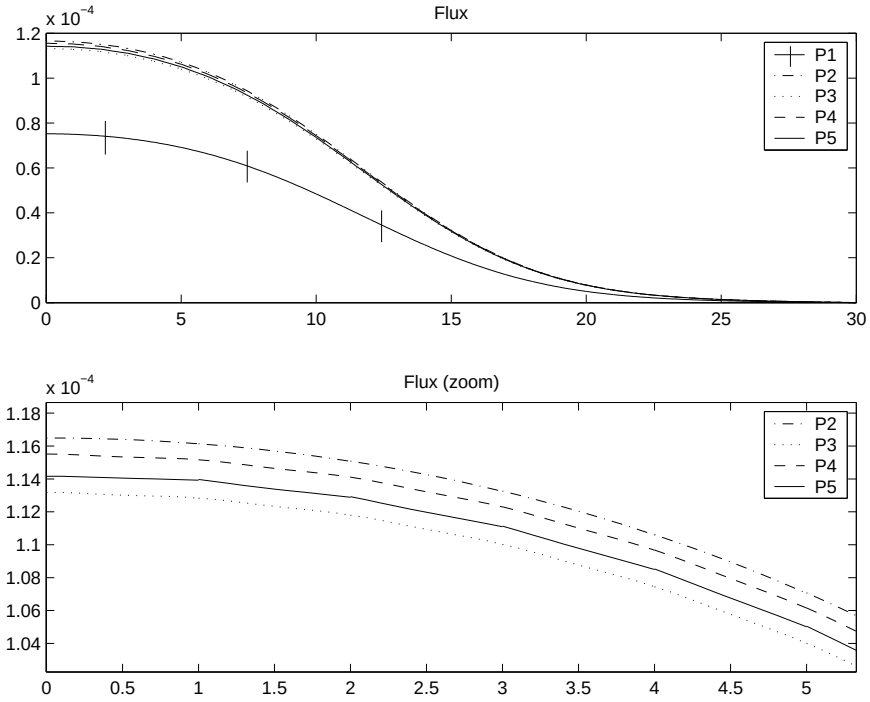

Figure 2: Primal flux at $y = 29.75$, as a function of x.

5 Conclusions

The mixed-hybrid methods have been applied to the within-group transport equation. Such methods combine attractive features of both mixed and hybrid methods, namely the simul-

[b] In fact, the coefficient of the highest spatial order vanishes for the current ($f_{-,l}(\mathbf{r})$), which thus ends up being of the fifth order. This can be motivated mathematically.

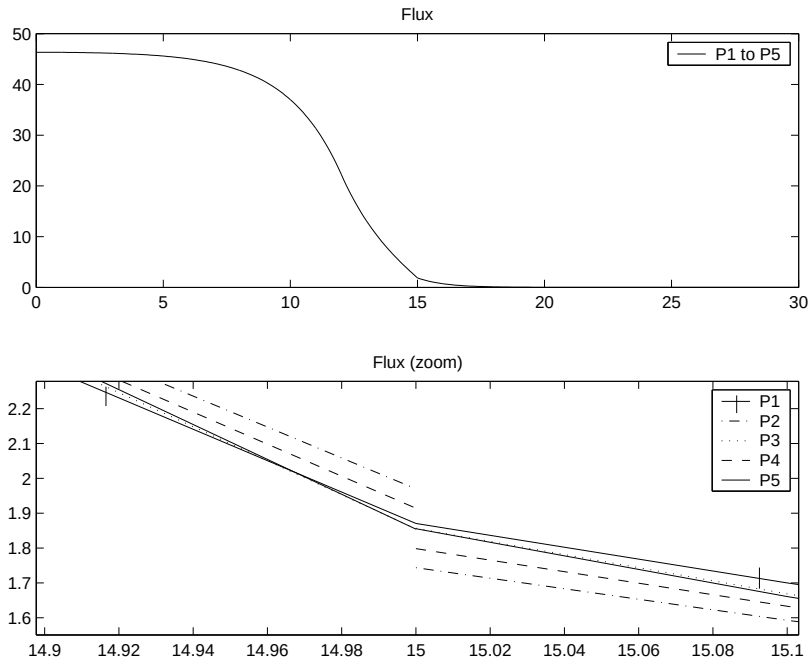

Figure 3: Primal flux at $y = 7.5$, as a function of x. Note the discontinuity of the even-order fluxes.

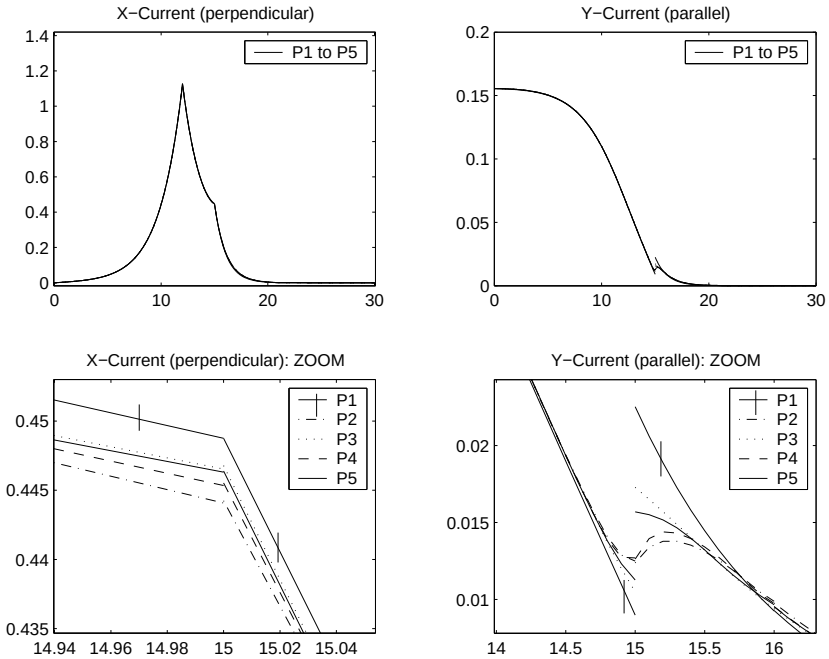

Figure 4: Primal currents at $y = 7.5$, as a function of x. Note the discontinuity of the odd-order Y-currents.

taneous approximation of even- and odd-parity fluxes (thus of flux and current) and the relaxation of interface continuity requirement using Lagrange multipliers. The distinction between primal and dual formulations, related to the spatial variable and therefore already present in diffusion, carries over into transport, where it interacts with the distinction between even- and odd-order spherical harmonics expansions.

Our numerical experiments illustrate the continuity properties of even- and odd-order P_N methods derived in section 3.2. These properties are the same in both primal and dual mixed-hybrid formulations. Furthermore, an enclosing behavior can be observed using both even- and odd-order P_N methods. While even-order methods have been widely employed, this work shows that even-order methods also offer significant potential in computational neutron transport.

An important area of future research is the development of an efficient solution technique for the linear system arising after discretization of our mixed-hybrid methods. This work nevertheless provides a global view of mixed-hybrid methods, supplying insight for the choice of a method even before the solving process is considered. Also, mixed-hybrid methods have been shown to be a way to generalize mixed methods from diffusion to transport.

Extension to multi-group transport with anisotropic scattering and source is under consideration. Further research also includes k_{eff} calculations.

Acknowledgement

This work was supported, in part, through Los Alamos National Laboratory contract 1152-001-00 4T/W-7405-E.

References

[1] E. Lewis, W. Miller, Jr., "Computational methods of neutron transport", John Wiley & Sons (1984).

[2] V. Vladimirov, "Mathematical problems in the one-velocity theory of particle transport", Tech. rep., Atomic Energy of Canada Ltd., Ontario (1963), translated from Transactions of the V.A. Steklov Mathematical Institute, **61** (1961).

[3] I. Babŭska, J. Oden, J. Lee, "Mixed-hybrid finite element approximations of second-order elliptic boundary-value problems", Computer methods in applied mechanics and engineering 11, pp. 175–206 (1977).

[4] C. de Oliveira, "An arbitrary geometry finite element method for multigroup neutron transport with anisotropic scattering", Progress in Nuclear Energy 18 (1/2), pp. 227–236 (1986).

[5] G. Palmiotti, E. Lewis, C. Carrico, "VARIANT: VARIational Anisotropic Nodal Transport for multidimensional cartesian and hexagonal geometry calculations", Tech. Rep. ANL-95/40, Argonne National Laboratory (1995).

[6] J. Lautard, D. Schneider, A. Baudron, "Mixed dual methods for neutronic reactor core calculations in the cronos system", in: Proc. Int. Conf. Mathematics and Computation, Reactor Physics and Environmental Analysis of Nuclear Systems, Madrid, Spain, Sept. 27-30, 1999, pp. 814–826 (1999).

[7] G. Rumyantsev, "Boundary conditions in the spherical harmonic method", Reactor Science and Technology (Journal of Nuclear Energy Parts A/B), 16, pp. 111–118 (1962).

[8] E. Lewis, C. Carrico, G. Palmiotti, "Variational nodal formulation for the spherical harmonics equations", Nuclear Science and Engineering 122 (2), pp. 194–203 (1996).

[9] Yang, "Rumyantsev interface conditions for P_N method", Argonne National Laboratory. Unpublished (2003).

[10] H. Khalil, "A nodal diffusion technique for synthetic acceleration of nodal S_N calculations", Nuclear Science and Engineering 90 (3), pp. 263–280 (1985).